



LBNL-43243
Preprint

ERNEST ORLANDO LAWRENCE BERKELEY NATIONAL LABORATORY

Dissociative Photoionization Dynamics of SF₆ by Ion Imaging with Synchrotron Undulator Radiation

Darcy S. Peterka, Musahid Ahmed, Cheuk-Yiu Ng,
and Arthur G. Suits

Chemical Sciences Division

May 1999

Submitted to
Chemical Physics Letters



REFERENCE COPY
Does Not Circulate
Bldg. 50 Library - Ref.
Lawrence Berkeley National Laboratory

LBNL-43243

Copy 1

DISCLAIMER

This document was prepared as an account of work sponsored by the United States Government. While this document is believed to contain correct information, neither the United States Government nor any agency thereof, nor the Regents of the University of California, nor any of their employees, makes any warranty, express or implied, or assumes any legal responsibility for the accuracy, completeness, or usefulness of any information, apparatus, product, or process disclosed, or represents that its use would not infringe privately owned rights. Reference herein to any specific commercial product, process, or service by its trade name, trademark, manufacturer, or otherwise, does not necessarily constitute or imply its endorsement, recommendation, or favoring by the United States Government or any agency thereof, or the Regents of the University of California. The views and opinions of authors expressed herein do not necessarily state or reflect those of the United States Government or any agency thereof or the Regents of the University of California.

**Dissociative Photoionization Dynamics of SF₆ by Ion
Imaging with Synchrotron Undulator Radiation**

Darcy S. Peterka, Musahid Ahmed, Cheuk-Yiu Ng,[†]
and Arthur G. Suits*

Chemical Sciences Division
Ernest Orlando Lawrence Berkeley National Laboratory
University of California
Berkeley, California 94720

[†]Ames Laboratory, United State Department of Energy, and
Department of Chemistry, Iowa State University, Ames, IA 50011

May 1999

*Corresponding author: email AGSUILTS@LBL.GOV

This work was supported by the Director, Office of Energy Research, Office of Basic Energy Sciences,
Chemical Sciences Division, of the U.S. Department of Energy under Contract No. DE-AC03-76SF00098.

(Submitted to Chemical Physics Letters)

Dissociative photoionization dynamics of SF₆ by ion imaging with synchrotron undulator radiation

Darcy S. Peterka, Musahid Ahmed, Cheuk-Yiu Ng[†] and Arthur G. Suits^{*}

*Chemical Sciences Division
Ernest Orlando Lawrence Berkeley National Laboratory
Berkeley, CA 94720 USA*

*[†]Ames Laboratory, United States Department of Energy, and
Department of Chemistry, Iowa State University, Ames, IA 50011*

ABSTRACT

The technique of photofragment imaging, widely used in the study of neutral photochemistry, has been adapted to use on a VUV undulator beamline at the Advanced Light Source, affording a new approach to the study of dissociative ionization processes. The technique allows direct inversion of the raw data to yield angular and translational energy distributions for the product ions. The method is here applied to study the dissociative ionization of SF₆ at photon energies from 15 to 28 eV. The experiment allows for detailed characterization of the angular and translational energy distributions of the fragments, providing insight into the decay mechanisms of these excited ionic states.

^{*} Corresponding author: email AGSUITTS@LBL.GOV

1. Introduction

The oscillator strength distribution of most molecules reaches a maximum in the vacuum ultraviolet (VUV)¹, and dissociative ionization is the principle decay mechanism following excitation of molecules in the VUV. Dissociative ionization is thus one of the most important photochemical processes. Dissociative ionization processes can illuminate features of ion-molecule reactions just as neutral photodissociation has been used to characterize some reactions in so-called "half-collision" experiments. Sophisticated approaches have been employed in recent years using coincidence methods^{2,3}, for example, to study dissociative ionization from energy selected ions. In general, these methods rely on analysis of the ion time-of-flight peak shape to characterize the kinetic energy released as well as the angular distributions for the process. These approaches achieve a precise definition of the initial state of the ion, but generally do not yield the full kinetic energy or angular distributions for the process of interest. We have recently adapted the ion imaging technique⁴ for use on the Chemical Dynamics Beamline, an undulator beamline at the Advanced Light Source⁵.

Ion imaging is a method that has recently seen wide application in neutral photochemistry, crossed-beam collision dynamics and reactive scattering⁶. The technique has the advantage that complete energy and angular distributions are recorded simultaneously, and the data analysis may be accomplished by direct inversion of the raw data. A closely related technique has been used by Eland and coworkers in a coincidence mode to look at three-body fragmentation processes in double ionization^{7,8}. In this first application of the ion imaging technique in conjunction with synchrotron radiation, the 'white beam' from the undulator is used with its inherent 2% bandwidth.

Studies of SF₆ dissociative ionization include early photoionization mass spectrometry measurements of partial ionization cross sections using both a helium continuum source⁹ and synchrotron radiation¹⁰ as well as electric dipole (e,e+ion) spectroscopy¹¹. In addition, an early photoelectron-photoion coincidence (PEPICO) study reported kinetic energy release for SF₆ through the \tilde{X} and \tilde{A} states¹². More recent studies have included negative ion mass spectrometry¹³, and both low-resolution¹⁴ and high-resolution¹⁵ PEPICO studies using synchrotron radiation. In the PEPICO study of Creasey et al., detailed dynamical information was inferred from average kinetic energy release measurements for SF₅⁺, SF₄⁺ and SF₃⁺ as well as onsets for the specific decay channels. Evans et al.¹⁵, using a supersonic molecular beam of SF₆ with a 6.65 m Eagle monochromator, measured high-resolution PEPICO TOF spectra for fragment ions from SF₆

dissociative ionization, with particular interest in the thermochemistry. Recently, Yench et al. reported a high-resolution threshold photoelectron spectroscopy study for SF₆ to 28 eV¹⁶. In this paper, we present preliminary results obtained on an imaging endstation on the Chemical Dynamics Beamline, characterizing the dissociative photoionization dynamics of SF₆ in a molecular beam, excited at energies from 15 to 28 eV.

2. Experimental

The experiments were performed in a new endstation recently added to the Chemical Dynamics Beamline. The apparatus is schematically illustrated in the inset to Fig. 1. Briefly, it features a molecular beam source pumped by a 2000 L/s magnetic bearing turbomolecular pump. The molecular beam is skimmed once before entering the ionization chamber, pumped by two 400 L/s magnetic bearing turbomolecular pumps. Product ions are accelerated by repeller and acceleration fields into a 0.5 meter flight tube perpendicular to the plane of the beams. They then strike a position-sensitive detector, which is a 40-mm diameter dual microchannel plate coupled to a phosphor screen (Galileo 3040FM). Photionization yield (PIY) spectra were obtained by integrating the ion TOF peaks as a function of photon energy. Mass-selected images were obtained by pulsing the microchannel plate, typically pulsing from a DC value of -1100 to -1900 V, with 300 nanosecond duration. The detector is viewed by an integrating fast-scan video camera system employing thresholding in conjunction with a linear video look-up table. Typical accumulation times were 10 minutes for each image.

The molecular beam was produced by passing neat SF₆ through a piezoelectric pulsed valve operating at 90 Hz with 100 microsecond pulses. Time-of-flight mass spectra were recorded by placing a photomultiplier tube to view the detector. The polarization of the undulator radiation is purely linear, and parallel to the plane of the detector. The images recorded are 2-dimensional projections of the 3-dimensional recoiling product ion sphere. The translational energy, speed and angular distributions were reconstructed from the projection using standard techniques⁶.

Images of SF₅⁺, SF₄⁺ and SF₃⁺ were recorded (when observed) at various photon energies from 16.0 to 24 eV. These are not coincidence experiments, and the dissociation processes are not presented for energy selected ions. However, to estimate contributions from particular electronic states, difference images were created during analysis. This involved collecting two images one below and one above the rise of a feature in the PIY curve and then subtracting them.

This approach is intended to provide an overview of the dynamics in a given region, but clearly does not yield truly energy-selected measurements. Analysis of the images was performed using the conventional inverse Abel transform to reconstruct the product-flux contour maps from the images, which are 2-dimensional projections of the 3-dimensional fragment distributions. These were then integrated radially and about the polar angle to yield the velocity and angular distributions, respectively.

3. Results

PIY Spectra

The PIY spectra for the various product ions are shown in Fig. 1. Arrows in the figure indicate photon energies at which images were recorded to obtain translational energy and angular distributions. The onset for SF_5^+ is found near 15.5 eV, consistent with previous reports (see ref. ¹⁷ and references) It shows additional onsets at 17 eV, 20 eV, some decrease beginning near 19 eV, and a very prominent resonant feature at 23 eV. SF_4^+ shows an onset around 18.5 eV, again consistent with previous reports, and shows only modest changes up to 30 eV. SF_3^+ appears at 20 eV, and exhibits the same resonant feature seen in SF_5^+ near 23 eV.

SF_5^+

Images for SF_5^+ at 16, 16.8, 17.6, and 23.2 eV are shown in Fig. 2a-d. From these images, we obtain the translational energy distributions shown in Fig. 3. These energy distributions show surprisingly little change with the changing excitation energy throughout this region. As mentioned above, these results are not obtained for energy-selected ions. Instead, we derive the translational energy distributions from difference images taken in an effort to isolate the contribution for a given region of onset. At 16 eV the average translational energy release is 0.62 eV, and extends to a maximum of 1.8 eV. At 16.8 and 17.6 eV the average release is ~0.55 eV with a maximum energy of 1.4 eV, while at 23.2 eV the average energy release is 0.66 eV with a maximum release of ~1.7 eV.

The angular distributions are shown for SF_5^+ for the four representative photon energies in Fig. 4. These were fitted to the familiar expression: $I(\Theta) \propto 1 + \beta P_2(\cos(\Theta))$ to obtain the β parameters¹⁸. The β values obtained are: 0.94 at 16 eV, 1.23 at 16.8 eV, 1.24 at 17.6 eV, and reach a maximum of 1.31 at 23.2 eV.

SF₄⁺ and SF₃⁺

Images recorded for SF₄⁺ at 19.5 and 21.3 eV and SF₃⁺ at 21.3 and 23.2 eV are shown in Fig. 2e-h. The thresholds for SF₄⁺ and SF₃⁺ production are around 18.5 eV and 19 eV respectively, consistent with previous reports. Since the co-fragments are not necessarily known, we present recoil speed distributions rather than total translational energy distributions. These are shown in Fig. 5, along with that obtained for SF₅⁺ at 16 eV for comparison. The corresponding angular distributions (not shown) are nearly isotropic for both SF₄⁺ and SF₃⁺ as can be seen in the data images.

4. Discussion

Previous studies of the PIY spectra for SF₆ were mainly conducted up to the He(I) line at 21.2 eV⁹, and our results are largely consistent with that previous work. More recently, Mitsuke et al.¹³, reported PIY measurements for SF₅⁺ and SF₃⁺ up to 31 eV in the course of studies of ion-pair formation. The dominant feature that appears in the energy range from 21 to 30 eV is the broad resonance evident in both the SF₅⁺ and SF₃⁺. This feature is not seen as prominently in the SF₄⁺ ion. It is believed that this feature represents a shape resonance arising from excitation to quasibound levels of the electron that are briefly trapped by a barrier formed from the electron density around the electronegative fluorine atoms¹⁹. Mitsuke et al. argue that this resonance is associated with a $5a_{1g} \rightarrow 6t_{1u}$ transition, which correlates to a $3s \rightarrow 3p$ transition on the central sulfur atom. The translational energy distributions for SF₅⁺ at this photon energy imply that much of the additional energy is taken away by the electron in the process of autoionization (otherwise the energy would exceed that permitting bound SF₅⁺.) Studying relying on coincidence with threshold electrons show no evidence of this feature^{16,20}, supporting the inference that it is associated with autoionization to lower lying ionic states.

The detailed kinetic energy distributions shown in Fig. 3 are the first obtained for dissociative photoionization of SF₆, and noteworthy in the level of detail achieved. The average of the distributions agree reasonably well with the low resolution measurements previously reported^{17,21}. These distributions are remarkably independent of ionization energy, possibly suggesting a late barrier to decomposition of SF₆⁺ to SF₅⁺ + F. Consideration of the geometry changes involved provides a plausible picture of the dissociation pathway. Stretching of one of the S-F bonds in SF₆⁺ yields an SF₅⁺ ion initially in a square pyramidal geometry¹². However, recent

ab initio calculations^{22,23} confirm that the structure of SF₅⁺ is clearly trigonal bipyramidal (D_{3h}), so that extensive rearrangement must occur during the dissociation process. The kinetic energy release likely reflects fairly efficient conversion of the energy of this barrier into product repulsion. The fact that the kinetic energy distributions are similar for several excited states of the SF₆⁺ ion may suggest that internal conversion to the ground state of the ion precedes dissociation. This is also consistent with the similarities in the angular distributions.

The angular distributions in the figures represent the first at this level of detail for a dissociative ionization event, although Powis and coworkers^{24,25} have investigated these and related phenomena through examination of ion time-of-flight peak shapes. Our observed anisotropic SF₅⁺ angular distributions augment the picture of the dynamics sketched above. All of the SF₅⁺ distributions show considerable anisotropy consistent with a parallel dissociation; that is, the fragments show a strong tendency to dissociate on an axis parallel to the polarization of the VUV radiation. This may seem surprising for such a highly symmetrical molecule (point group O_h.) Ionization through the \tilde{X} , \tilde{A} and \tilde{B} states of SF₆⁺ are (1t_{1g}⁻¹) and [(5t_{1u}⁻¹)+(1t_{2u}⁻¹)] ionizations respectively¹⁷. These all represent removal of 2p lone pair electrons from the fluorine atoms⁹, so it is perhaps not so surprising that a more local view of the ionization and subsequent dissociation is appropriate. The angular distributions further show that the autoionization via the shape resonance must be very rapid. Photoelectron spectra at these photon energies would be useful to identify the SF₆⁺ state(s) formed in the ionization step. All of these angular distributions show that the SF₆⁺ dissociation is very rapid, occurring on a timescale short compared to its rotational period

The threshold for SF₄⁺ production appears near the onset of the \tilde{C} state of SF₆⁺ at 18 eV. It has long been concluded, based on this coincidence and the absence of any apparent influence of the onset of this state on the SF₅⁺ yield, that the SF₄⁺ originates as the exclusive product the SF₆⁺ \tilde{C} state dissociation^{9,17}; since this is nominally below the threshold for formation of SF₄⁺ + F + F, it has been argued that \tilde{C} state dissociation exclusively yields SF₄⁺ + F₂. Recent calculations show that this appearance energy is actually above the threshold for SF₄⁺ + F + F²³. In fact, the remarkable similarities in the SF₄⁺ recoil speed distribution to that of SF₅⁺ at lower energy (see Fig. 5) suggest a picture in which the primary product is SF₅⁺ + F throughout this region, including the \tilde{C} state. This is supported by the relative insensitivity of the SF₅⁺ translational energy distributions

to the photon energy, implying that the bulk of the excess energy remains in the SF_5^+ when the photon energy is increased. If it is assumed that the initial step produces SF_5^+ with an average of 0.7 eV translational energy, then secondary decomposition of the SF_5^+ to $SF_4^+ + F$ will become dominant (replacing the SF_5^+ production) at about 18.8 eV. Any residual long-lived SF_5^+ in this region will be found only for the relatively small contribution from the fastest (lowest internal energy) SF_5^+ product. This is precisely what is seen in the PIY curves in Fig. 1.

The angular distributions for SF_4^+ are, within experimental error, isotropic; however, this is difficult to compare directly to SF_5^+ because there is so little SF_5^+ production at the photon energies where SF_4^+ appears. The absence of anisotropy may simply reflect the difference in the orientation of the electronic transition moment with respect to the bond axis, or it may be a consequence of the lifetime of the SF_5^+ prior to decomposition, or perhaps both. For SF_4^+ at the higher photon energies accessing the \tilde{E} state, however, much of the additional photon energy is coupled effectively into translational energy of the SF_4^+ product. At these higher energies accessing the \tilde{D} and \tilde{E} states, we may be seeing a shift to nonstatistical energy partitioning, or we may have internal conversion to the \tilde{A} , \tilde{B} states giving a distinct translational energy distribution for the SF_4^+ product there.

The SF_3^+ begins to appear around 19 eV, consistent with previous reports. Again for the SF_3^+ however, we see a velocity distribution remarkably similar, at least in the location of the peak, to the SF_5^+ at energies where it is a principal product. The SF_3^+ angular distributions are isotropic, and the velocity distributions change only modestly with photon energy in this region. Fig. 5 shows the SF_3^+ velocity distribution compared to that of SF_4^+ at the same energy. Again, there is an increase as the photon energy is increased, but perhaps the most striking feature of all of these distributions is their similarity. This is consistent with the picture outlined above in which the translational energy release in the primary step, yielding $SF_5^+ + F$, is the principle feature in all of these distributions, and subsequent fluorine atoms are lost sequentially as the energy is available. Future studies will exploit the imaging technique in conjunction with energy-selected electrons to define the initial state of the ion.

Acknowledgements

We thank Dr. B. Ruscic for helpful discussions, Mr. D. Chen for assistance in preliminary studies, and acknowledge assistance from the ALS staff. This work was supported by the Director, Office of Energy Research, Office of Basic Energy Sciences, Chemical Sciences Division of the U.S.

Department of Energy under contract No. DE-ACO3-76SF00098. The ALS is supported by the Director, Office of Energy Research, Office of Basic Energy Sciences, Materials Sciences Division of the U.S. Department of Energy under the same contract.

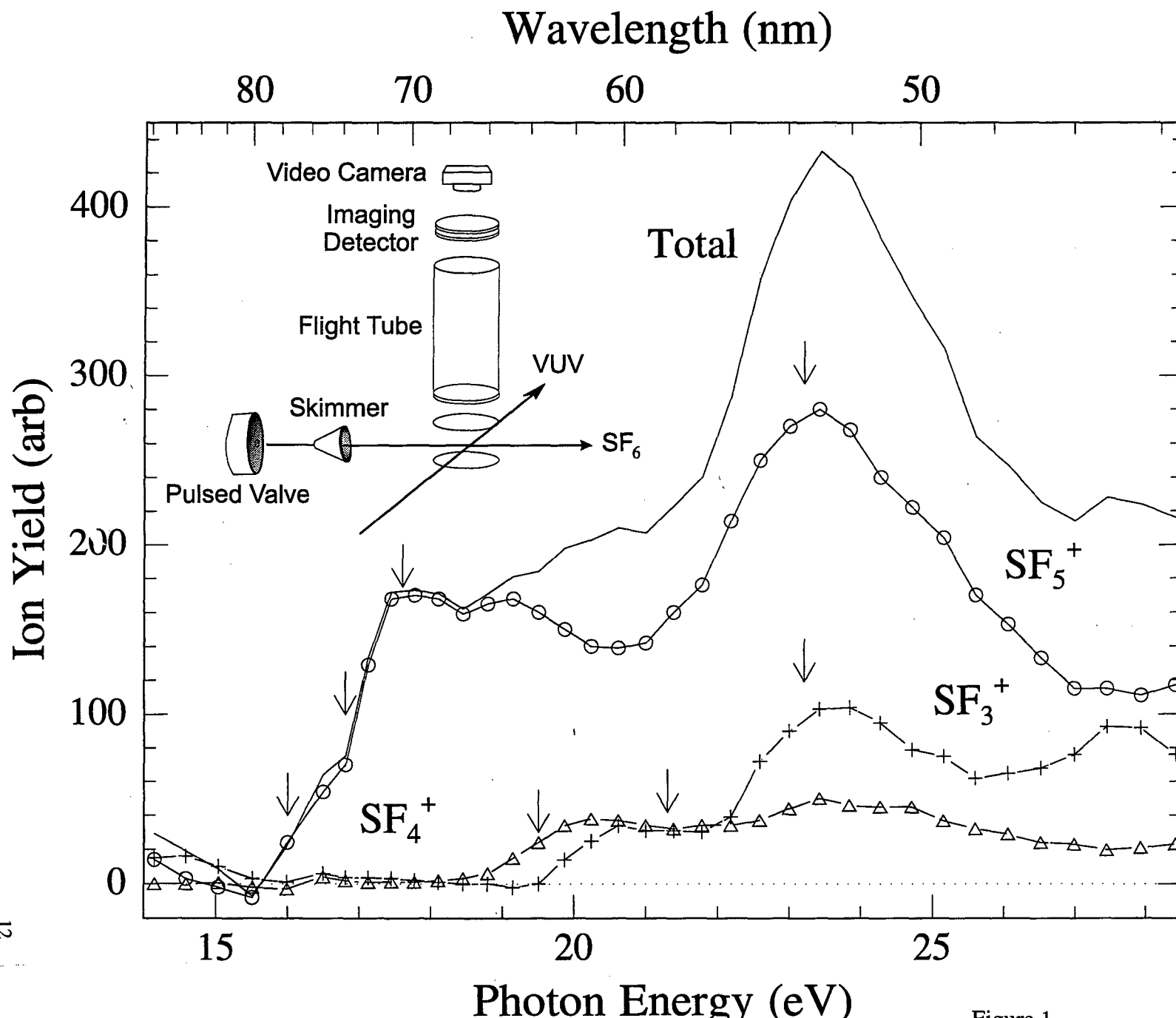
Figure Captions

1. Photoion yield spectra for SF₆. Inset shows a schematic view of the imaging endstation.
2. A-D: SF₅⁺ data images at the indicated photon energy: A) 16 eV B) 16.8-16 eV C) 17.6-16.8 eV D) 23.2-21.3 eV. E-H: data images for the following product ion and photon energy: E) SF₄⁺ 19.5 eV; F) SF₄⁺ 21.3 eV G) SF₃⁺ 21.3 eV; H) SF₃⁺ 23.2 eV.
3. Total translational energy distributions for the images shown in Fig. 3 A-D.
4. Angular distributions obtained from the images in Fig. 3A-D.
5. Recoil speed distributions for the following fragments and photon energies A) solid line, SF₄⁺ 19.5 eV; dashed line, SF₄⁺ 21.3 eV; dot-dash line, SF₅⁺ 16 eV. B) solid line, SF₃⁺ 21.3 eV; dashed line, SF₃⁺ 23.2 eV.

REFERENCES

- 1 Y. Hatano, in *Dynamics of Excited Molecules*, edited by K. Kuchitsu (Elsevier, 1994), pp. 151-216.
- 2 C. Y. Ng, in *Vacuum Ultraviolet Photoionization of Photodissociation of Molecules and Clusters*, edited by C. Y. Ng (World Scientific, Singapore, 1991), pp. 169.
- 3 T. Baer, J. Booze, and K. M. Weitzel, in *Vacuum Ultraviolet Photoionization of Photodissociation of Molecules and Clusters*, edited by C. Y. Ng (World Scientific, Singapore, 1991), pp. 259.
- 4 D. W. Chandler and P. L. Houston, *J. Chem. Phys.* 87 (1987) 1445.
- 5 P. A. Heimann, M. Koike, C. W. Hsu, D. Blank, X. M. Yang, A. G. Suits, Y. T. Lee, M. Evans, C. Y. Ng, C. Flaim, and H. A. Padmore, *Rev. Sci. Instrum.* 68 (1997) 1945-1951.
- 6 A. J. R. Heck and D. W. Chandler, *Ann. Rev. Phys. Chem.* 46 (1995) 335-372.
- 7 S. Hsieh and J. H. D. Eland, *Rapid Commun. Mass Spectrom.* 9 (1995) 1261.
- 8 S. Hsieh and J. H. D. Eland, *J. Phys. B* 30 (1997) 4515.
- 9 J. Berkowitz, *Photoabsorption, Photoionization and Photoelectron Spectroscopy* (Academic Press, New York, 1979).
- 10 M. Sasanuma, E. Ishiguro, H. Masuko, Y. Morioka, and M. Nakamura, *J. Phys. B* 11 (1975) 3655.
- 11 A. P. Hitchcock and M. J. V. d. Viel, *J. Phys. B* 12 (1979) 2153.
- 12 I. G. Simm, C. J. Danby, J. H. D. Eland, and P. I. Mansell, *J. Chem. Soc. Farad. Trans. II* 72 (1976) 426.
- 13 K. Mitsuke, S. Suzuki, T. Imamura, and I. Koyano, *J. Chem. Phys.* 93 (1990) 8717.
- 14 J. C. Creasey, I. R. Lambert, R. P. Tuckett, K. Condling, L. J. Frasinski, P. A. Hatherly, M. Stankiewicz, and D. M. P. Holland, *J. Chem. Phys.* 93 (1990) 3295.
- 15 M. Evans, C. Y. Ng, C. W. Hsu, and P. Heimann, *J. Chem. Phys.* 106 (1997) 978-981.
- 16 A. J. Yencha, D. B. Thompson, A. J. Cormack, D. R. Cooper, M. Zubek, P. Bolognesi, and G. C. King, *Chem. Phys.* 216 (1997) 227.

- 17 J. C. Creasey, I. R. Lambert, R. P. Tuckett, K. Condling, L. J. Frasinski, P. A. Hatherly, and M. Stankiewicz, *J. Chem. Soc. Faraday Trans.* 87 (1991) 1287.
- 18 R. N. Zare, *Mol. Photochem.* 4 (1972) 1.
- 19 J. L. Dehmer, *J. Chem. Phys.* 56 (1972) 4496.
- 20 K.-M. Weitzel, C. Y. Ng, and et al., (Unpublished results).
- 21 J. C. Creasey, H. M. Jones, D. M. Smith, R. P. Tuckett, P. A. hatherly, K. Coding, and I. Powis, "*Chem. Phys.*", 174 (1993) 441,.
- 22 Y. S. Cheung, W. K. Li, S. W. Chiu, and C. Y. Ng, *J. Chem. Phys.* 101 (1994) 3412-3413.
- 23 Y. S. Cheung, Y. J. Chen, C. Y. Ng, S. W. Chiu, and W. K. Li, *J. Am. Chem. Soc.* 117 (1995) 9725-9733.
- 24 K. G. Low, P. D. Hampton, and I. Powis, *Chem. Phys.* 100 (1985) 401.
- 25 I. Powis, O. Dutuit, M. Richard-Viard, and P. M. Guyon, *J. Chem. Phys.* 92 (1990) 1643.



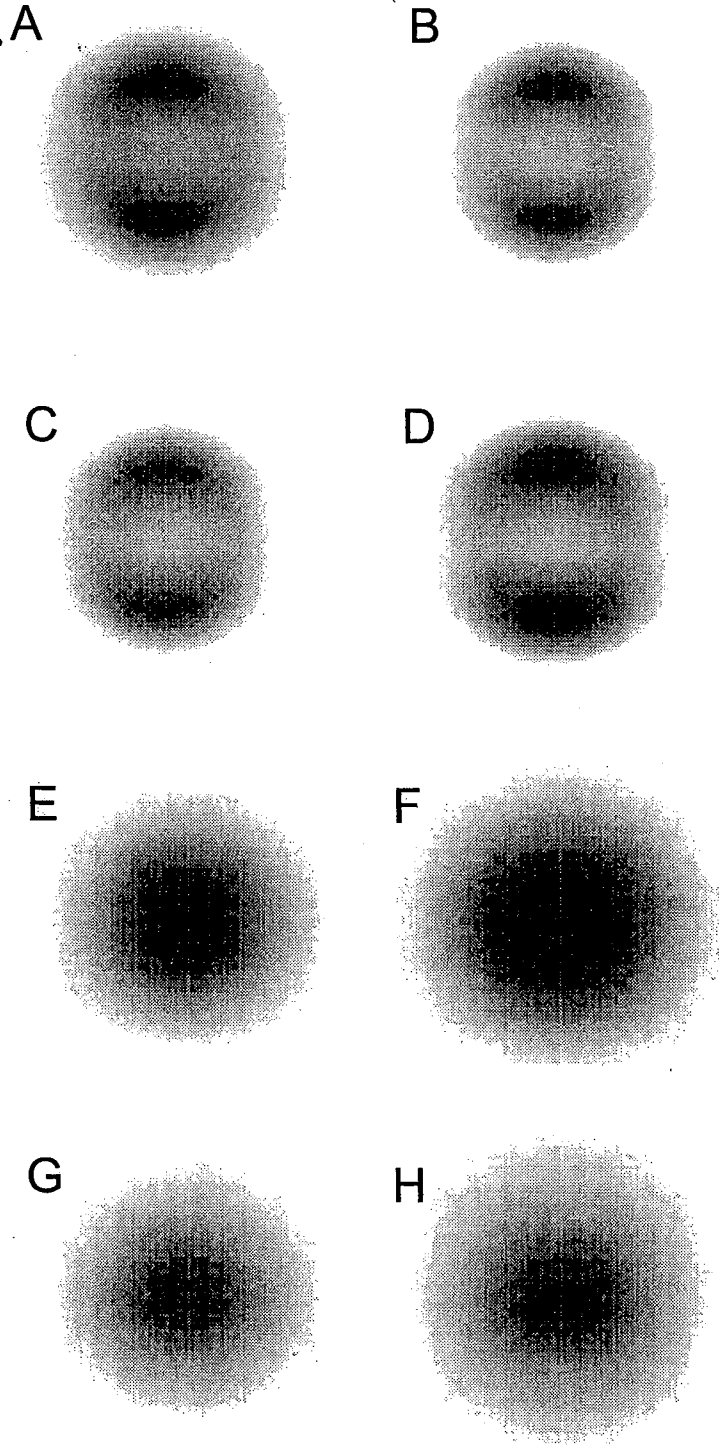


Figure 2

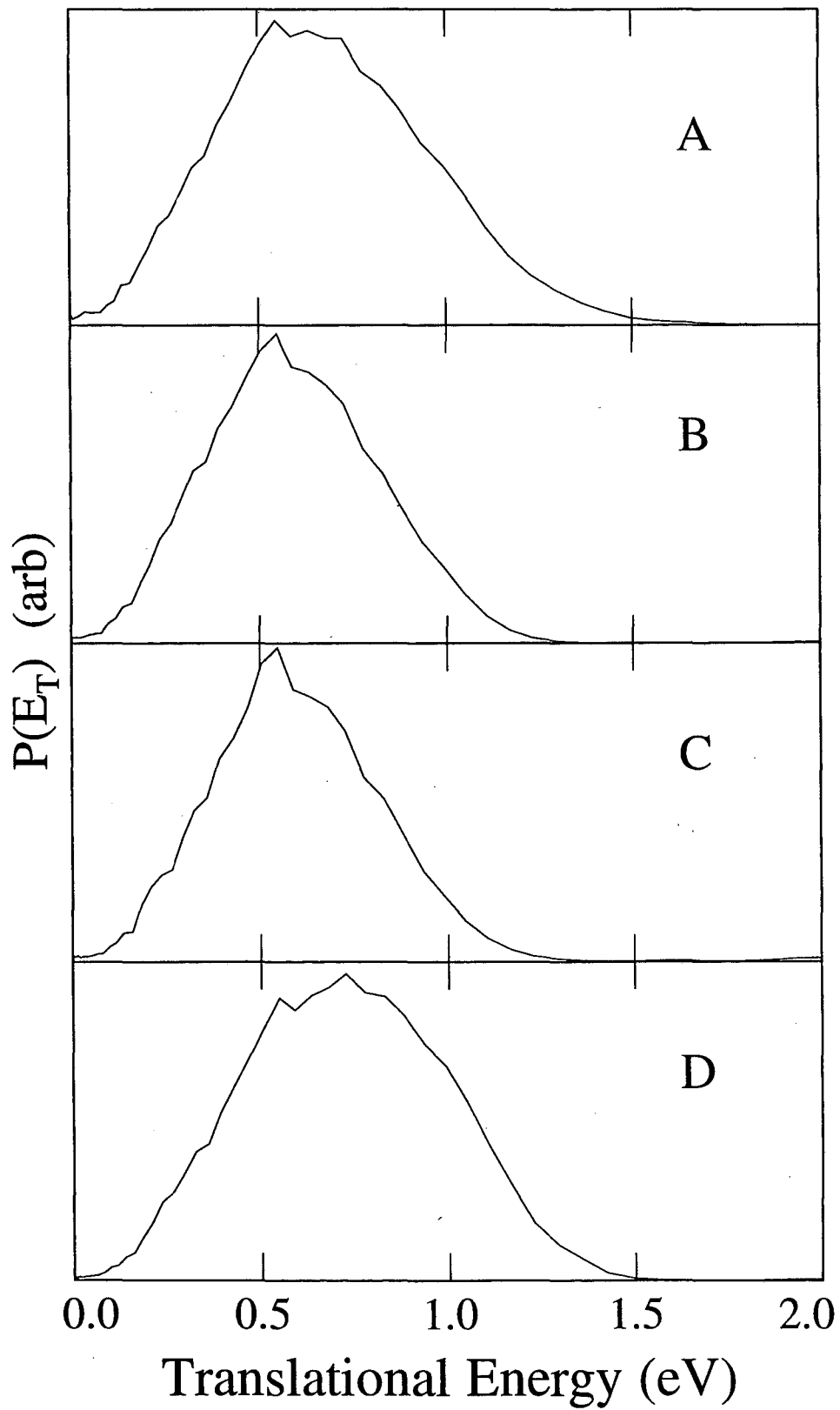


Figure 3

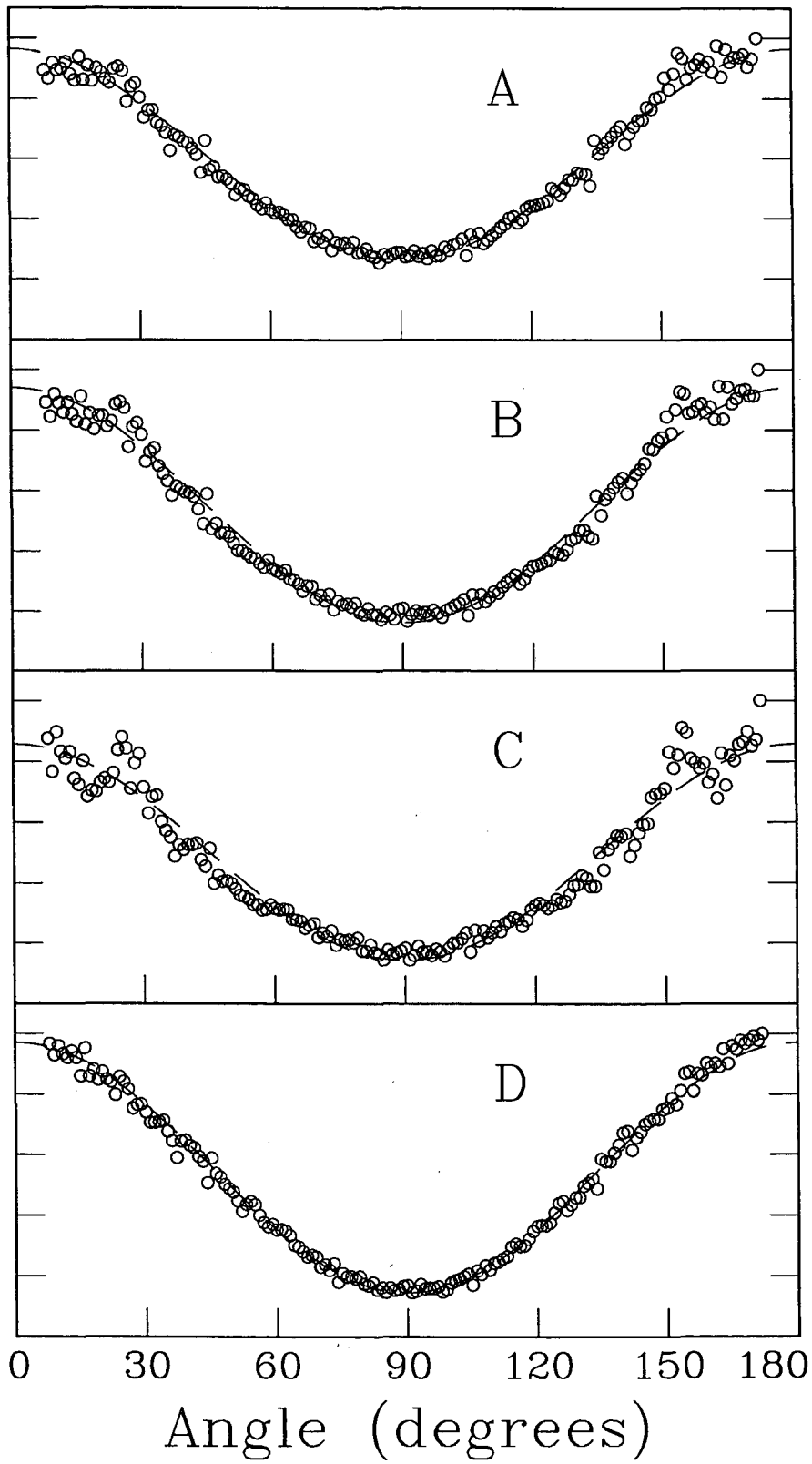


Figure 4

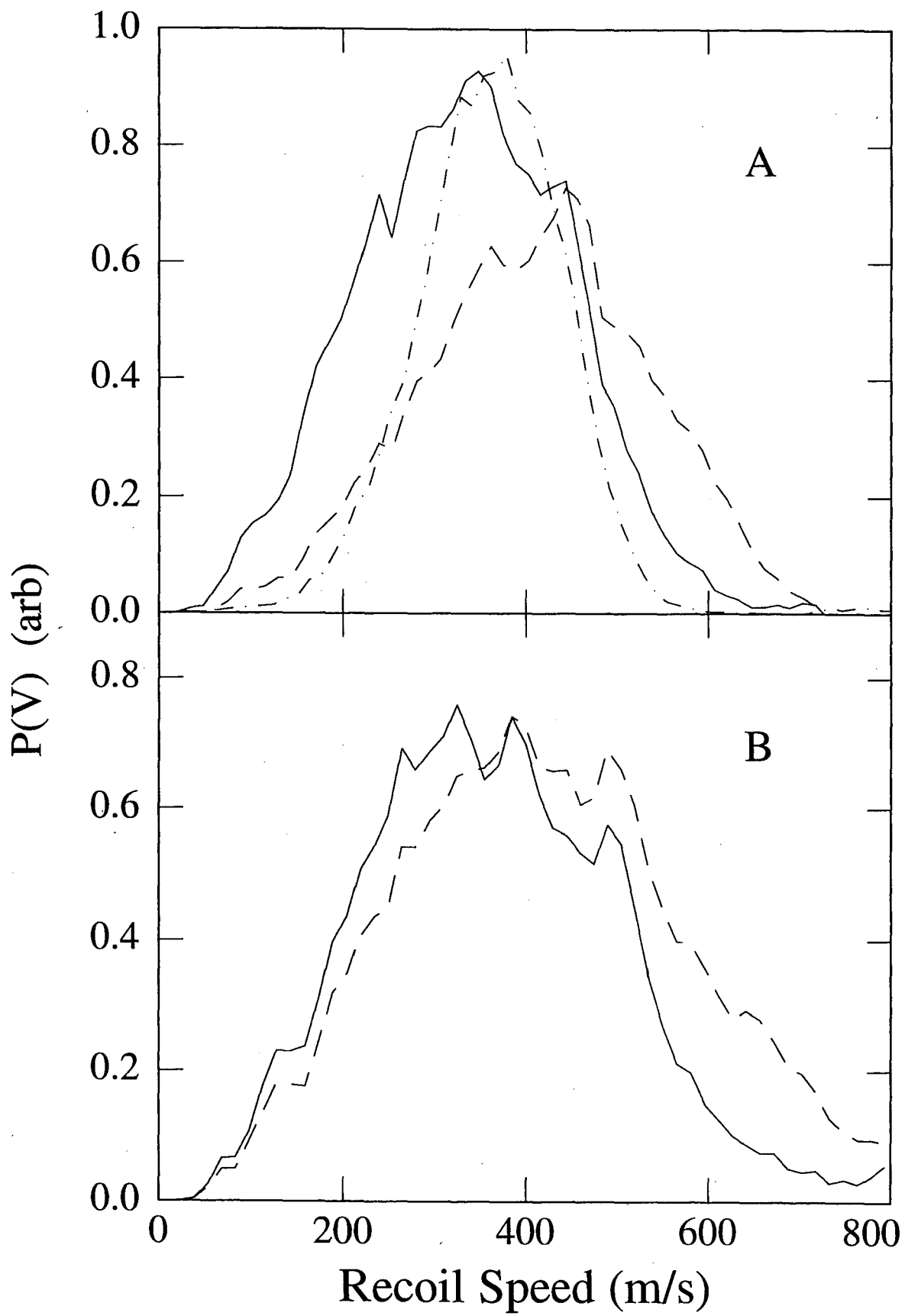


Figure 5

**ERNEST ORLANDO LAWRENCE BERKELEY NATIONAL LABORATORY
ONE CYCLOTRON ROAD BERKELEY, CALIFORNIA 94720**